ACS SENSORS

pubs.acs.org/acssensors
Article

Probiotic Antimicrobial Evaluation Via Real-Time Profiling of Bacterial Cell Proliferation Using Stochastic Kinetics

Seong-Geun Jeong,*,▽ Youjin Lee,▽ Hye-Seon Jeong,▽ Seong Jun Park, Jinki Yeom, Chang-Hyung Choi, and Byung-Gee Kim

Cite This: ACS Sens. 2025, 10, 1880−1888
Read Online

ACCESS | Metrics & More | Article Recommendations | Supporting Information

ABSTRACT: Probiotic metabolites are gaining attention as potential antibiotic candidates against antibiotic-resistant bacteria. The disk diffusion test, by measuring bacterial aggregate responses, faces challenges in accurately evaluating antimicrobial efficacy when these responses to different probiotic strains are indistinguishable at a macroscopic level. Here, this study presents an analytical method for accurately evaluating antimicrobial activity by analyzing bacterial cell proliferation suppression at a microscopic level. This assay can be used in a coculture system, designed to continuously expose pathogenic bacteria growing on the bottom surface of the culture plate to probiotic metabolites, selectively released from porous capsules positioned above. Bacterial proliferation is optically monitored in real-time and tracked via a computer vision algorithm. Specifically, bacterial proliferation is quantified as their doubling time, calculated using a proposed stochastic kinetic model. This method identifies the most potent antimicrobial strains by determining which probiotic candidates most effectively extend the bacterial doubling time. In comparative experiments using the same strains, this proposed method demonstrated clear distinctions in the antimicrobial efficacy of each strain, unlike the disk diffusion test. Therefore, this approach provides a reliable solution for identifying superior probiotic strains, with potential for widespread use in discovering new antimicrobial agents.

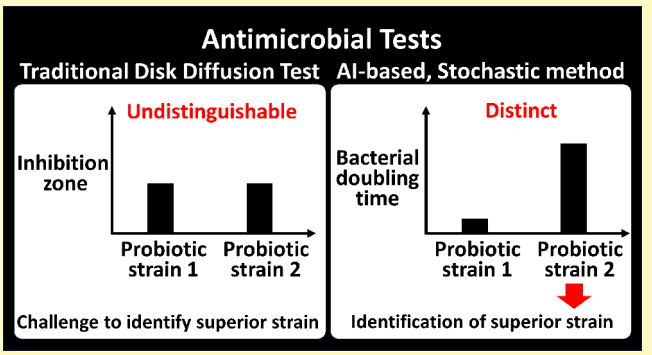

KEYWORDS: *antimicrobial tests, probiotics, stochastic kinetics, microcapsule, computer vision*

The rise of antibiotic-resistant bacteria has become a global health threat, driving the urgent need for alternative strategies to combat pathogenic microorganisms.[1−3] Among these alternatives, probiotics have emerged as promising candidates for developing new antimicrobial agents, owing to their ability to secrete bioactive metabolites, such as bacteriocins and organic acids, which suppress the growth of pathogenic bacteria.[4−6] Identifying the probiotic strain with the strongest antimicrobial properties is crucial for developing effective antimicrobial therapies.[7,8]

Traditional methods, such as the disk diffusion test, have been widely used to evaluate antimicrobial efficacy by measuring the size of the inhibition zone where bacterial growth is suppressed.[9,10] However, this method is influenced by factors such as the diffusivity of the compounds being tested in agar.[11−13] These factors can mask the true antimicrobial potential of probiotic strains, as differences in potency may not be accurately reflected in the inhibition zone.[14] In particular, the macroscopic responses of bacterial aggregates can lead to multiple strains exhibiting similar inhibition zone sizes, making it difficult to distinguish their true antimicrobial effects (Figure 1A). Consequently, while useful for initial screening, this approach lacks the accuracy required for identifying the most potent strains.[15−17] Therefore, beyond analyzing macroscopic bacterial responses, more advanced assays are needed—by analyzing microscopic bacterial responses—to accurately characterize the antimicrobial activity of probiotics and select the optimal strains for therapeutic development.[18,19]

To address this limitation, this study presents an analytical method for accurately validating antimicrobial activity by analyzing bacterial cell proliferation suppression at a microscopic level (Figure 1B). This assay can be used in a coculture system, designed to continuously expose pathogenic bacteria growing on the bottom surface of the culture plate to probiotic metabolites, which are selectively released from porous capsules positioned above. The developed computer vision algorithm directly counts individual bacterial cells over time,

Received: October 27, 2024
Revised: January 22, 2025
Accepted: February 18, 2025
Published: February 27, 2025

https://doi.org/10.1021/acssensors.4c03003
ACS Sens. 2025, 10, 1880−1888

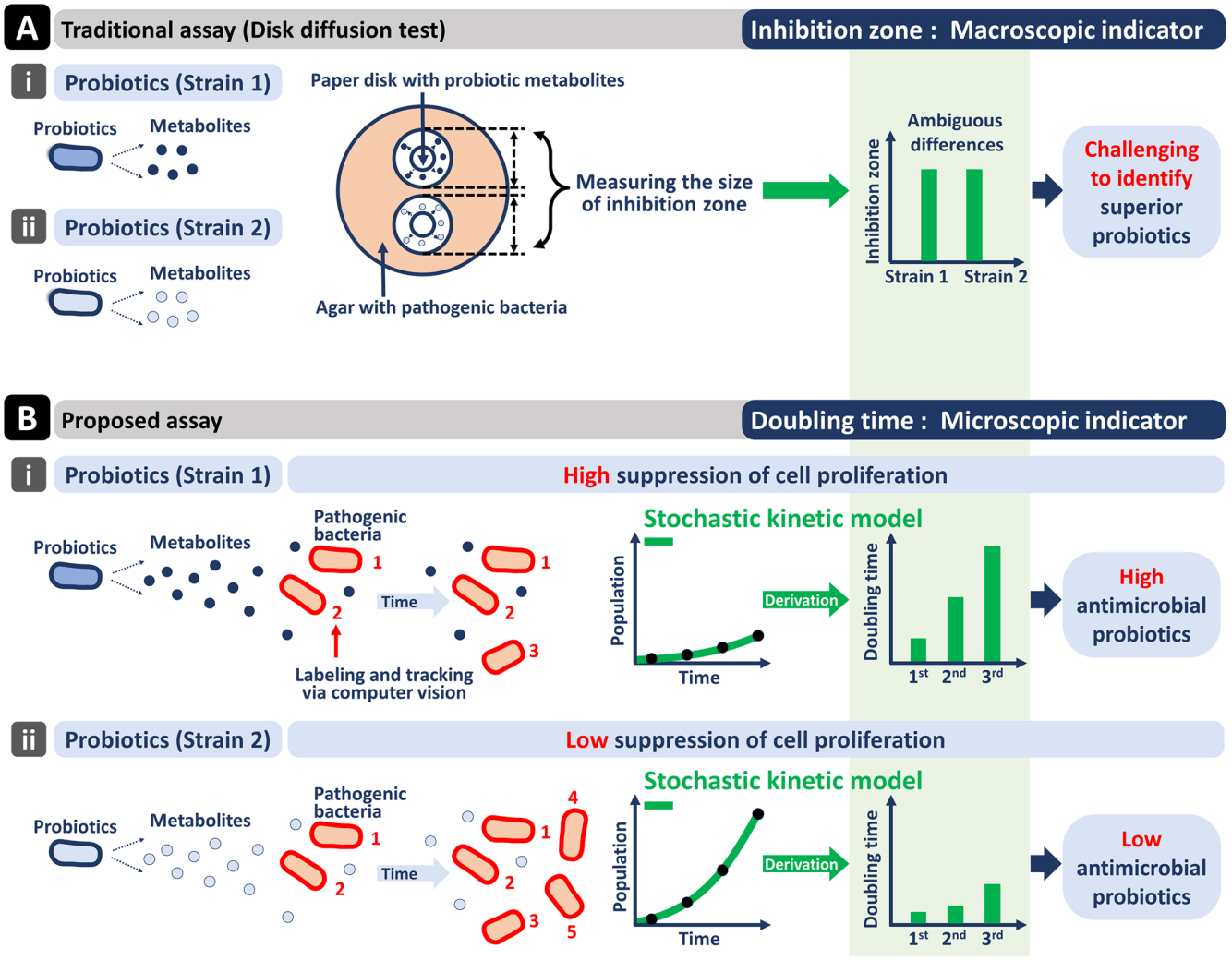

Figure 1. Cellular-level, stochastic assay vs Disk diffusion test. (A) Disk diffusion test. This traditional test measures the inhibition zones of pathogenic bacteria around probiotic metabolites. Both probiotic strains (strain 1 and strain 2) produce similar size of inhibition zones, making it challenging to distinguish the superior strain. (B) Cellular-level, stochastic assay. This assay identifies high antimicrobial probiotic strains using computer vision and stochastic kinetics. The pathogenic bacteria are exposed to metabolites of different probiotics separately (i,ii). The bacterial population is tracked using computer vision, which labels individual bacterial cells in real-time (i.e., 1, 2, 3...) and continuously counts the cells. A stochastic kinetic model then calculates the doubling time based on the bacterial population data. A longer doubling time indicates higher antimicrobial activity, reflecting suppression of pathogenic bacterial proliferation. (i) Strain 1 exhibits a longer doubling time than (ii) strain 2, suggesting that strain 1 is the higher antimicrobial strain. This stochastic test identifies superior antimicrobial strains by using the doubling time as a metric of antimicrobial activity.

enabling precise detection of pathogenic bacterial proliferation and its suppression by probiotics.[20,21] Specifically, bacterial proliferation is quantified as the doubling time, calculated using a stochastic kinetic model. Longer bacterial doubling time indicates greater suppression of bacterial proliferation, suggesting stronger antimicrobial efficacy of the probiotic strain. Leveraging this relationship, this method identifies the most potent antimicrobial strains by determining which probiotic candidates most effectively extend the bacterial doubling time.

The proposed microscopic method significantly reduces the time required to detect bacterial proliferation suppression compared to traditional macroscopic methods (Table S1). Traditional methods, such as the disk diffusion test and optical density (OD) measurements, evaluate bacterial responses at the population level, limiting their ability to detect subtle suppression effects on bacterial proliferation caused by probiotic metabolites.[22,23] Consequently, these methods often require prolonged incubation times to generate reliable results.[24] In contrast, the proposed method directly counts bacterial cells at the single-cell level, enabling the detection of subtle proliferation suppression within shorter incubation times.

In comparative experiments using the same strains, the proposed method allows for the accurate identification of the most potent antimicrobial strain within a short time (≤4 h), unlike traditional methods (≥24 h).[25,26] The proposed method, which employs a microscopic metric, bacterial doubling time, enables more accurate antimicrobial evaluation compared to traditional methods that rely on macroscopic metrics such as inhibition zones or optical density. Therefore, this approach provides a reliable solution for accurately identifying superior antimicrobial strains in a short time, with promising potential for discovering new antimicrobial agents.

https://doi.org/10.1021/acssensors.4c03003
ACS Sens. 2025, 10, 1880−1888

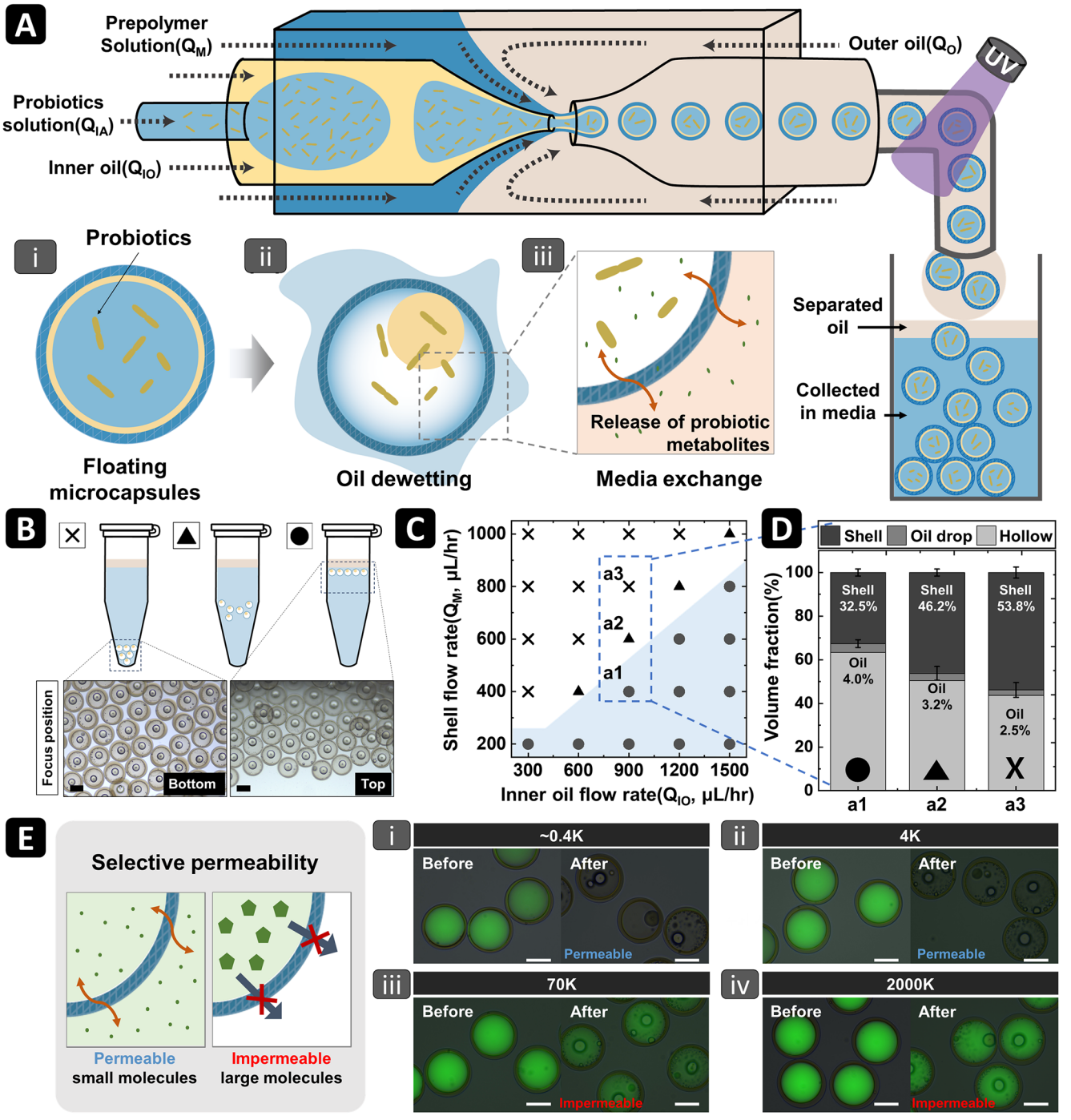

Figure 2. Microfluidic production of floatable hydrogel microcapsules containing probiotics. (A) The schematic showing the procedure of producing uniform hydrogel shell-microcapsules via photopolymerization using triple emulsions in a microfluidic device; (i) the probiotics are successfully encapsulated within microcapsules, and (ii) even after dewetting of the oil layer due to osmotic shock, the probiotics are retained inside without leakage, (iii) while the microcapsules are designed to selectively release only low-molecular-weight substances secreted by the probiotics. (B) Photographs and corresponding micrographs showing that the capsules can float depending on the proportion of oil present within the capsules. (C) The phase diagram of the volumetric flow rates of oil and prepolymer phases illustrates the region where floatable microcapsules can be produced. (D) Plot showing the volume fractions of oil and the hydrogel shell within the capsules under three representative volumetric flow rate conditions in the phase diagram. (E) Schematic diagrams and corresponding composite micrographs illustrate the selective permeability of hydrogel microcapsules based on molecular weight. Fluorescent tracers (FITC-dextran) smaller than 4 kDa (i,ii) can permeate the hydrogel shell, whereas those larger than 70 kDa (iii,iv) are unable to pass through. All scale bars are 100 μm.

RESULT AND DISCUSSION

Microfluidic Production of Floating Hydrogel Microcapsules Containing Probiotics. The triple emulsion drop-based microfluidic technique is demonstrated to enable the production of floatable microcapsules containing probiotics, as illustrated in the schematic diagram in Figure 2A. The triple emulsion drops are prepared using a capillary microfluidic device, with the fabrication procedure detailed in the

https://doi.org/10.1021/acssensors.4c03003
ACS Sens. 2025, 10, 1880−1888

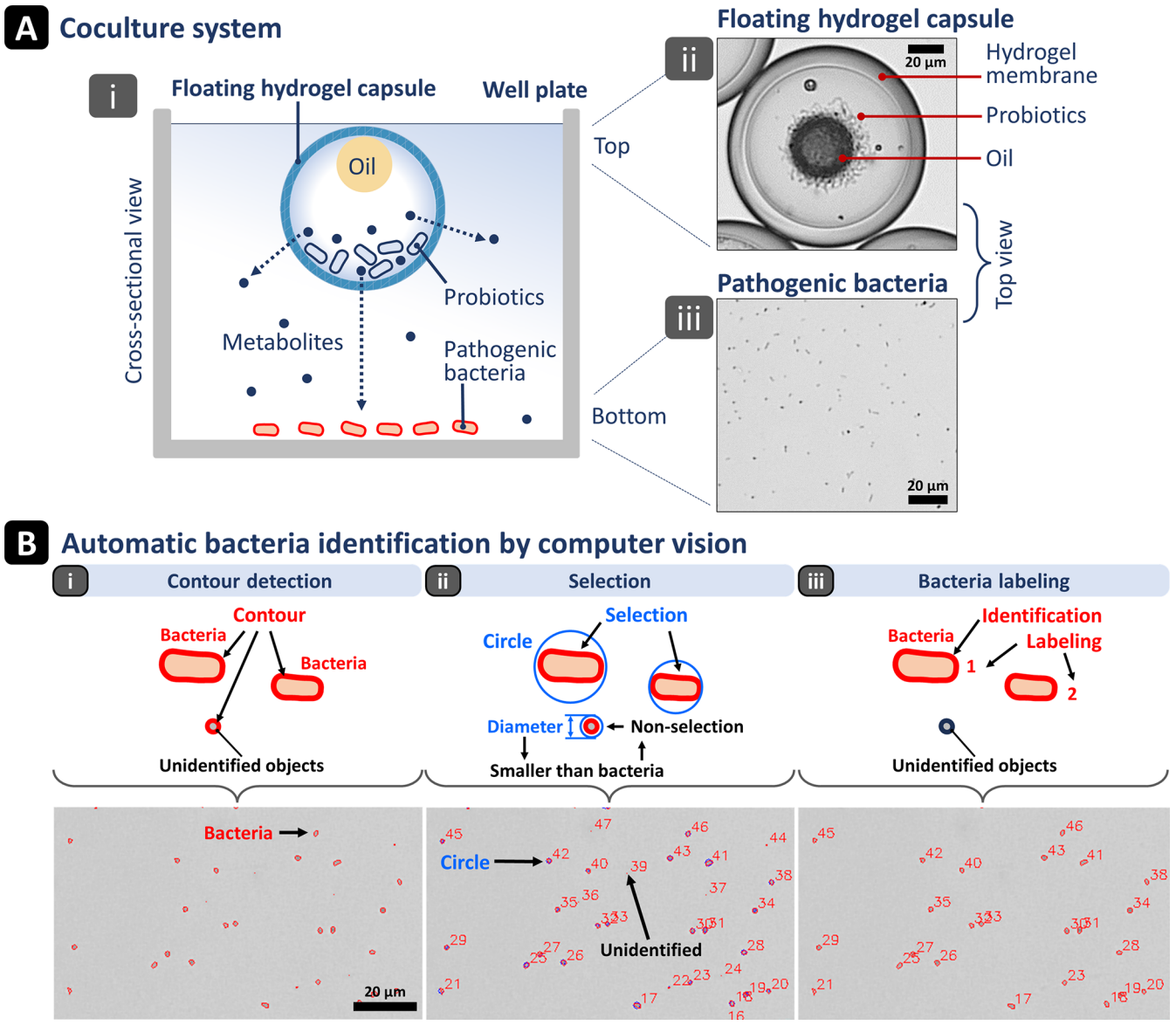

Figure 3. Coculture system and bacteria identification by computer vision. (A) Coculture system setup. (i) Cross-sectional view of the floating hydrogel microcapsule system. The oil droplet inside the microcapsule allows it to float at the top of the medium, positioning the probiotics at the top and pathogenic bacteria at the bottom of the medium. This separation allows selective tracking of bacterial proliferation at the bottom of the medium without fluorescent labeling or staining to distinguish the bacteria. (ii) Top view of the floating hydrogel microcapsule containing probiotics at the top of the medium. (iii) Top view of the pathogenic bacteria at the bottom of the medium. (B) Bacteria identification by computer vision. The computer vision-based algorithm selectively identifies and labels pathogenic bacteria in the medium, where pathogenic bacteria and similarly shaped microscale objects coexist, potentially leading to misidentification in automated analysis. The algorithm first identifies object contours in microscopic images (i). Objects with diameters smaller than the average bacterial size are excluded (ii). Finally, the bacterial objects are labeled with unique ID numbers for tracking (iii), allowing for real-time tracking of bacterial proliferation in time-lapse images.

Experimental Section. To form the triple emulsion drops, an aqueous media solution with probiotics (IW) is introduced through the smaller tapered capillary to form the innermost core. For example, the aqueous hydrogel prepolymer solution of polyethylene glycol diacrylate (PEGDA, 10%) and 1% photoinitiator (Darocur1173) can be used. An oil phase (hexadecane with 2% Span80, IO) is introduced with the aqueous media solutions with probiotics through the injection capillary. This coaxial biphasic stream, formed in the injection capillary, generates a periodic flow of aqueous media solution droplets within the oil phase, facilitated by the preferential wetting of the oil phase on the hydrophobically treated inner wall of the injection capillary. This flow behavior facilitates the formation of a thin lubrication oil layer between the innermost aqueous media solutions drop and the hydrophobic wall of the injection capillary. Next, an additional hydrogel prepolymer solution (M) is introduced through the interstices between the injection capillary and the square capillary. The triphasic fluid stream is sheared by an outer oil phase (mineral oil with 2.5 wt % Span80, O) at the entrance of the collection capillary, forming uniform triple emulsion drops with a thin oil layer, as shown in Figure 2A. These triple emulsion drops are exposed to UV illumination, allowing hydrogel microcapsules with an intermediate oil layer (Figure 2A-i). By maintaining the oil layer within the capsule at a temperature below its freezing point for a short period, it undergoes dewetting from the

https://doi.org/10.1021/acssensors.4c03003
ACS Sens. 2025, 10, 1880−1888

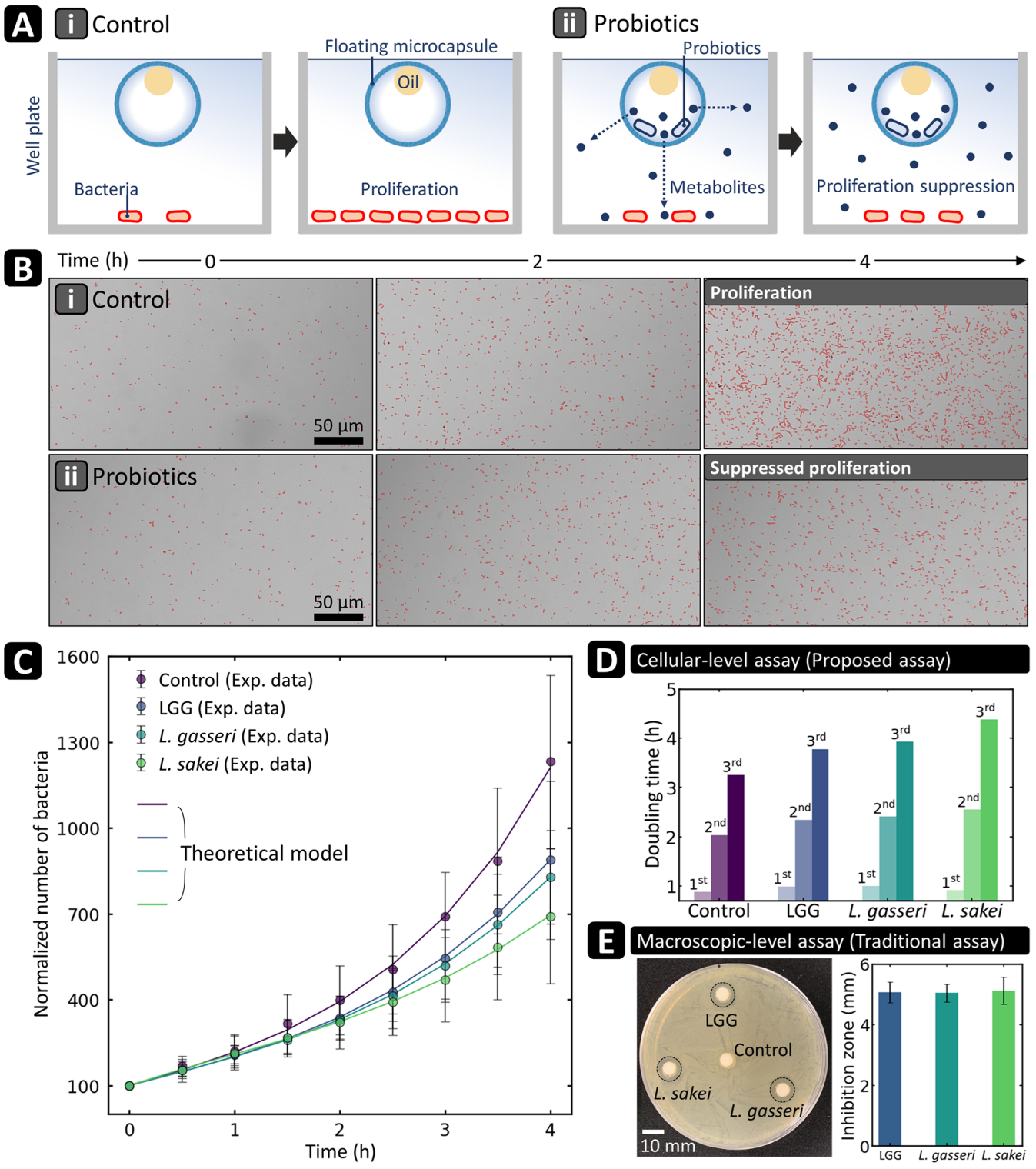

Figure 4. Evaluation of probiotic antimicrobial activity using a cellular-level assay and disk diffusion test. (A) Schematic representation of the cellular-level assay using (i) an empty microcapsule (control) and (ii) a probiotic-loaded microcapsule. (B) Time-lapse images of bacterial proliferation. (i) In the control group, bacterial proliferation progresses rapidly over 4 h. (ii) In the presence of probiotics metabolites, bacterial proliferation is suppressed, as demonstrated by the antimicrobial activity of metabolites. (C) Bacterial proliferation and stochastic kinetic model. Proliferation curves show the normalized number of bacteria over time for control, LGG, *L. gasseri*, and *L. sakei* strains. A stochastic kinetic model is fitted to the experimental data, which is used to calculate the doubling time of all strains. (D) Doubling time analysis. *L. sakei* exhibits the longest doubling times, followed by *L. gasseri* and LGG, indicating stronger suppression of bacterial proliferation. This assay identifies the superior strain by analyzing the doubling time. (E) Disk diffusion test. This traditional test shows similar inhibition zones (~5 mm) for all strains, thereby challenging to identify the superior strain among candidates.

https://doi.org/10.1021/acssensors.4c03003
ACS Sens. 2025, 10, 1880−1888

hydrogel shell.[27] This process ensures the probiotics are encapsulated, while their secreted substances can diffuse out (Figure 2A-ii). During this process, the probiotics are retained within the capsule, while the substances secreted by the probiotics are designed to be released through the shell (Figure 2A-iii). The microcapsules generated from the microfluidic device can be engineered to settle at the bottom, disperse uniformly, or float at the top of the medium, depending on the volumetric flow rate conditions of the fluids used (Figure 2B and Table S2). The phase diagram, depicted by the volumetric flow rates of the inner oil phase and prepolymer phase, indicates the region where the production of floatable particles is feasible (Figure 2C). To understand the mechanisms underlying the floatability of the microcapsules, the volume fractions of specific regions within microcapsules formed under three representative flow rate conditions presented in the phase diagram were analyzed (Figure 2D). These results confirm that as the volume fraction of low-density oil within the capsule increases, the overall density of the capsule becomes lower than that of the medium, enabling the capsule to float. To evaluate the permeability of the proposed microcapsule shell, FITC-tagged dextran with various molecular weights was encapsulated as a fluorescent tracer, and the release of these molecules after oil dewetting was investigated. As shown in Figure 2E, the 4 kDa fluorescent tracer permeated through the shell, while tracers of 70 kDa (D_h = 4.6 nm) and larger remained confined within the capsule. This demonstrates that although the probiotics are securely retained, the antimicrobial agents they secrete can easily diffuse out.

Encapsulated Probiotic-Pathogen Coculture System. To investigate the antimicrobial efficacy of probiotics on pathogenic bacterial proliferation at the cellular level, a coculture system with the probiotics and pathogenic bacteria is proposed (Figure 3A). This system features the coculturing of encapsulated probiotics and pathogenic bacteria in the same medium but at different locations; the microcapsules float at the top of the medium, while the pathogenic bacteria settle at the bottom (Figure S1). The secretions from the probiotics inside the capsule are continuously released through the hydrogel membrane, exposing the pathogenic bacteria at the bottom to these secretions. The proliferation of pathogenic bacteria is monitored and imaged in real-time. This setup simplifies the distinction between bacteria from probiotics without requiring fluorescent labeling or staining, allowing selective time-lapse imaging of bacterial growth, which facilitates the analysis of bacterial proliferation over time. Moreover, the metabolites produced by the probiotics diffuse through the permeable membrane of the microcapsule into the medium, interacting with the pathogenic bacteria and enabling the investigation of the antimicrobial efficacy of the probiotics on bacterial growth.

Tracking Bacterial Proliferation via Computer Vision. The computer vision algorithm was developed to track bacteria proliferation at the cellular level (Figure 3B). First, the algorithm identifies the contours of all microscale objects, including bacteria, in the microscopic images (Figure 3B-i). Second, a circle is fitted to the contour of each object, and the diameter of each object is measured (Figure 3B-ii). Microscale objects with diameters smaller than the average bacterial contour diameter are excluded in the selection group (Figure S2). This step prevents errors caused by misidentifying smaller microscale objects as bacteria. Finally, after minimizing errors by excluding nonbacterial objects, the remaining bacterial objects are labeled (e.g., 1, 2, 3...) for tracking (Figure 3B-iii). This automatic labeling algorithm enables accurate and simple counting individual bacterial cells on time-lapse images, thereby allowing for the tracking of bacterial proliferation over time.

Antimicrobial Evaluation via Stochastic Kinetics of Cell Proliferation. To assess the performance of the proposed assay, the antimicrobial efficacy of three probiotics—*Lactobacillus rhamnosus* GG (LGG), *Lactobacillus gasseri* (*L. gasseri*), and *Lactobacillus sakei* (*L. sakei*)—was evaluated by analyzing the proliferation of pathogenic bacteria exposed to metabolites from probiotics-loaded microcapsules. Figure 4A represents a schematic overview of the experimental setup, showing how empty microcapsules (control) or probiotics-loaded microcapsules influence the proliferation of pathogenic bacteria. To ensure accurate evaluation and minimize resource competition between probiotics and pathogenic bacteria (*Escherichia coli*), mixed media (50% MRS, 50% LB) was applied to the well plate. MRS supports probiotic growth but is less favorable for *E. coli*, whereas LB supports the growth of *E. coli* but is less favorable for probiotics (see the section "Optimizing coculture environments" in the Supporting Information).[28,29] Under empty microcapsules, bacteria proliferate without suppression, whereas metabolites released from probiotics-loaded microcapsules effectively suppress bacterial proliferation. Time-lapse images were captured to track bacterial proliferation (Figure 4B). The red contours, identified by the computer vision algorithm, indicate bacterial cells in each image. Under empty microcapsules, the number of red contours increased significantly over time, reflecting rapid bacterial proliferation in the absence of probiotics (Figure 4B-i). Conversely, under microcapsules with *L. sakei*, the increase in the number of red contours was much less pronounced, demonstrating the efficacy of the probiotics in suppressing bacterial proliferation (Figure 4B-ii).

The bacterial population data over time was quantified by counting bacteria from the time-lapse images for the three strains: *Lactobacillus rhamnosus* GG (LGG), *Lactobacillus gasseri* (*L. gasseri*), and *Lactobacillus sakei* (*L. sakei*) (Figure 4C). A proliferation curve was generated for each condition (control, LGG, *L. gasseri*, and *L. sakei*), showing the normalized number of bacteria over time. It is challenging to perfectly match the initial bacterial counts across all experimental conditions, thereby the initial bacterial population was normalized to 100 for all conditions to ensure a consistent comparison. The results clearly show a distinct suppression of bacterial proliferation in the presence of probiotics. In the control, the bacterial population increased significantly over time, whereas, in the presence of all three probiotics, the increase in bacterial population was significantly lower compared to the control. In particular, *L. sakei* exhibited the strongest suppression of bacterial proliferation, indicating its superior antimicrobial efficacy. This demonstrates that the proposed assay can effectively identify the most potent probiotic strain within a short assay time (~4 h).

To quantify the suppression of bacterial proliferation, the bacterial population data from the time-lapse images was analyzed using our proposed stochastic kinetic model. This theoretical model calculates bacterial doubling times, providing a quantitative measure of proliferation suppression. The mathematical expression for the model is as follows (the detailed derivation of this model is described in the Supporting Information)

https://doi.org/10.1021/acssensors.4c03003
ACS Sens. 2025, 10, 1880−1888

$$\langle n(t)\rangle = n_0 \frac{\gamma e^{-kt} - 2k e^{-(\gamma-k)t}}{\gamma - 2k} \quad (1)$$

where t is time, n_0 is the initial bacterial population, γ is the cell decay rate, and k is the cell division rate. The proposed model fitted well to the experimental data, accurately capturing changes in bacterial populations over time (Figure 4C). Specifically, it calculated bacterial doubling times, providing an accurate, microscopic metric of the probiotics' antimicrobial efficacy. Doubling time refers to the duration required for the bacterial population to double. The first doubling time was measured as the duration required for the initial population (n_0) to double ($2\ n_0$). The second and third doubling times are the durations for the population to grow from $2\ n_0$ to $4\ n_0$ and $4\ n_0$ to $8\ n_0$, respectively. A longer doubling time indicates stronger suppression of bacterial proliferation, reflecting greater antimicrobial efficacy. *L. sakei* exhibited the longest doubling time, suggesting the strongest suppression of bacterial proliferation, followed by *L. gasseri* and LGG (Figure 4D). This method also revealed that *L. sakei* exhibits the strongest antimicrobial efficacy by significantly suppressing the growth of bacterial aggregates at the microscopic level, more than others (Figure S4). These results demonstrate that the proposed assay enables the identification of the most effective probiotic strain.

In addition, the doubling time provides a standardized metric for quantitatively assessing the antimicrobial effect of pathogenic bacterial growth suppression.[30] Comparing bacterial counts at arbitrary time points may offer a simple approach for evaluating probiotic antimicrobial effects. However, this method lacks standardization due to variability in the selection of reference time points. Moreover, comparisons at specific time points fail to reflect the entire growth curve and are vulnerable to distortion caused by experimental errors. In contrast, the doubling time is calculated by the stochastic kinetic model, which considers the entire growth curve, making it a standardized metric for quantitatively comparing antimicrobial effects.

The stochastic kinetic model provides not only the doubling time but also additional parameters such as the bacterial cell division rate (k) and the bacterial cell death rate (γ) (Table S3). These parameters theoretically explain how the interplay of the mean time required for cell division ($1/k$) and the mean time for cell survival ($1/\gamma$) affects the doubling time. For instance, *L. sakei* exhibits the highest $1/k$ and lowest $1/\gamma$ among the tested probiotics, correlating with its most extended third doubling time, which reflects the strongest suppression of bacterial growth. Therefore, the proposed model provides additional theoretical insights into bacterial cell dynamics.

In comparative experiments using the same strains, the traditional disk diffusion test failed to differentiate their antimicrobial efficacy, as all produced similar sizes of inhibition zones around 5 mm (Figure 4E). The size of the inhibition zone serves as a macroscopic metric of antimicrobial efficacy, but it may not accurately reflect true antimicrobial efficacy. Therefore, the proposed method, using the microscopic metric of doubling time, provides a more reliable approach for discovering the most potent probiotic strain, compared to the traditional method, which relies on the macroscopic metric of inhibition zone size.

Furthermore, the proposed microscopic method significantly reduces evaluation time compared to traditional macroscopic methods, such as the disk diffusion test and optical density (OD) measurement (Table S1). These macroscopic methods require prolonged incubation (≥24 h) to generate reliable assessments.[31] In contrast, the proposed method sensitively measures bacterial count changes at the single-cell level and accurately evaluates the antimicrobial efficacy rankings of three probiotics within a short incubation period (≤4 h). Therefore, the proposed method offers a reliable solution for accurately identifying superior probiotic strains in a short time, with promising potential for broad application in the discovery of new antimicrobial agents.

CONCLUSION

The proposed assay accurately identifies probiotics with superior antimicrobial activity by measuring the doubling time of pathogenic bacterial proliferation suppressed by probiotic metabolites. Specifically, the proposed stochastic kinetic model enabled accurate measurement of doubling time, allowing clearer differentiation of antimicrobial efficacy among probiotic strains. Additionally, the integration of hydrogel microcapsules with a computer vision algorithm enables label-free, real-time monitoring of pathogenic proliferation, eliminating the need for fluorescent tagging or staining.[32] By using doubling time as a microscopic antimicrobial metric, this assay offers a reliable solution for discovering superior probiotic strains that may be overlooked by traditional methods relying on macroscopic metrics such as the inhibition zone. Therefore, the stochastic assay has broad potential for discovering probiotic candidates in academic research and for antimicrobial agent development in industry.

EXPERIMENTAL SECTION

Antimicrobial Evaluation Procedure. The proposed assay begins by encapsulating each of the three probiotic strains into floating hydrogel microcapsules. These microcapsules, which contain probiotics, are then introduced into a well plate, followed by the addition of pathogenic bacteria into the medium. The floating design of the microcapsules ensures that the probiotics remain at the top of the medium, while the pathogenic bacteria settle at the bottom, allowing for selective observation of bacterial proliferation. This spatial separation between the probiotics and pathogenic bacteria eliminates the need for fluorescent labeling or staining to distinguish between them, which are of similar morphology. Therefore, by simply focusing the microscope on the bottom of the medium, time-lapse images of only the pathogenic bacteria are captured. Next, the computer vision algorithm, developed in Python, is applied to these images to recognize and track the bacterial population over time. Using this population data, the proposed stochastic kinetic model calculates bacterial doubling times. The probiotic strain that causes the longest doubling time in pathogenic bacteria is identified as the most effective antimicrobial strain.

Real-Time Live Cell Imaging in Incubation System. The culture well plate is placed in an incubator (Incubator T Series, Live Cell Instrument, Republic of Korea), set to supply 5% carbon dioxide and maintain a temperature of 37 °C. Then, 100 μL of floating microcapsules containing different probiotics are injected into each well, followed by the addition of 100 μL of media culture containing pathogenic bacteria. Time-lapse images are captured every 30 min at 10× or 20× magnification using a microscope (Eclipse Ti2, Nikon, Japan).

Computer Vision-Based Tracking of Bacterial Proliferation. The captured time-lapse images are analyzed using a Python-based algorithm that identifies object outlines and measures areas. The algorithm selectively recognizes bacteria in the time-lapse images, labeling new individual bacteria as they multiply. Over time, the algorithm automatically tracks bacterial numbers. The mean, standard deviation, and variance of bacterial counts and area over time are

https://doi.org/10.1021/acssensors.4c03003
ACS Sens. 2025, 10, 1880−1888

calculated from 12 different time-lapse images for each probiotic strain.

Preparation of Probiotics and Pathogenic Bacteria. The *Lacticaseibacillus rhamnosus* GG (LGG), *Lactobacillus gasseri* (*L. gasseri*), *Latilactobacillus sakei* (*L. sakei*) strains were inoculated into de Man, Rogosa, and Sharpe (MRS) medium (Difco, USA) and cultured in anaerobiosis at 37 °C for 48 h. After incubation, 2 mL of the culture broth was centrifuged at 4000*g* for 10 min, and the supernatant was collected. The pathogenic strain *E. coli* KCTC 2571 was incubated at 37 °C for 24 h in Luria−Bertani (LB) medium (Sigma-Aldrich, Saint Louis, MO, USA). For encapsulation of probiotics, the optical density (OD_{600}) of each probiotic strain was measured and standardized to 0.5 (equivalent to approximately 2.5×10^8 CFU/mL) to ensure a uniform concentration prior to encapsulation.

Materials for Microcapsule Fabrication. Polyethylene glycol diacrylate (PEGDA, Mn 700), 2,2-dimethoxy-2-phenylacetopheonon (photoinitiator), mineral oil, fluorescein isothiocyanate-dextran (Mw 2,000,000), Span 80 (Sorbitan monooleate, viscosity 1000−2000 mPa s (20 °C)), hexadecane (99%), trichloro(octadecyl)silane were purchased from Sigma-Aldrich. The FITC and FITC-tagged dextran (Sigma-Aldrich) were used to study the permeation property of microcapsules. 2-[Methoxy(polyethyleneoxy)propyl]trimethoxyl silane was purchased from Gelest. Deionized (DI) water (EXL 18.2 MΩ cm at 28 °C) was used for all aqueous solutions. Square glass capillaries with an inner diameter of 1.05 mm were purchased from Atlantic International Technology (A.I.T.) and cylindrical glass capillaries with inner diameter of 0.58 mm and outer diameter of 1.00 mm were purchased from World Precision Instruments Inc. (W.P.I.). Five min epoxy (Devcon) was used for assembling the glass capillary microfluidic devices.

Fabrication and Operation of Glass Capillary Microfluidic Device. The injection capillary is prepared by tapering a glass capillary with a 580 μm inner diameter (circular cross-section) down to a 100 μm inner diameter. To render the inner wall hydrophobic, the capillary is dipped in trichloro(octadecyl)silane for 10 min and then rinsed with ethanol. The injection capillary is inserted into a square capillary with an inner width of 1.05 mm, slightly larger than the injection capillary's outer diameter of 1 mm. Subsequently, a small tapered glass capillary (20 μm outer diameter) is prepared by pulling a cylindrical capillary; this small capillary is inserted into the injection capillary for coinjection of two immiscible fluids (innermost and inner phases). Finally, a tapered collection capillary (inner diameter of orifice: 350 μm) is inserted into the square capillary from the opposite end. The collection capillary is also treated with trichloro(octadecyl)-silane to make the capillary wall hydrophobic. During droplet generation, the volumetric flow rate is precisely controlled using syringe pumps (Legato100, KD Scientific), and the production of emulsion droplets is monitored with an inverted fluorescence microscope. During droplet generation, the volumetric flow rate is precisely controlled within a range of 100−10000 μL/h using syringe pumps (Legato100, KD Scientific), and the production of emulsion droplets is monitored using an inverted fluorescence microscope (Eclipse Ti2, Nikon) equipped with a high-speed camera (MINI UX 50). After droplet formation, the resulting hydrogel microcapsules were further characterized using the same microscope, now equipped with a CCD camera (sCMOS Zyla, Andor). Image analysis of the particles was performed using ImageJ to evaluate capsule morphology, size distribution, and dewetting behavior over time.

■ ASSOCIATED CONTENT

Supporting Information

The Supporting Information is available free of charge at https://pubs.acs.org/doi/10.1021/acssensors.4c03003.

Derivation of a stochastic kinetic model of cell proliferation, supporting figures (PDF)

■ AUTHOR INFORMATION

Corresponding Author

Seong-Geun Jeong − *Bio-MAX Institute, Seoul National University, Seoul 08826, Republic of Korea;* orcid.org/0000-0003-1968-4468; Email: hagnos@snu.ac.kr

Authors

Youjin Lee − *Department of Biomedical Sciences, College of Medicine, Seoul National University, Seoul 03080, Republic of Korea*

Hye-Seon Jeong − *School of Chemical Engineering, Yeungnam University, Gyeongsan, Gyeongbuk 38541, Republic of Korea*

Seong Jun Park − *National CRI-Center for Chemical Dynamics in Living Cells, Chung-Ang University, Seoul 06974, Republic of Korea; Department of Physics and Astronomy and Center for Theoretical Physics, Seoul National University, Seoul 08826, Republic of Korea*

Jinki Yeom − *Department of Biomedical Sciences, College of Medicine, Seoul National University, Seoul 03080, Republic of Korea; Department of Microbiology and Immunology, College of Medicine, Seoul National University, Seoul 08826, Republic of Korea*

Chang-Hyung Choi − *School of Chemical Engineering, Yeungnam University, Gyeongsan, Gyeongbuk 38541, Republic of Korea;* orcid.org/0000-0002-7561-3720

Byung-Gee Kim − *Bio-MAX Institute, Seoul National University, Seoul 08826, Republic of Korea; School of Chemical and Biological Engineering and Institute of Molecular Biology and Genetics, Seoul National University, Seoul 08826, Republic of Korea;* orcid.org/0000-0002-3776-1001

Complete contact information is available at: https://pubs.acs.org/10.1021/acssensors.4c03003

Author Contributions

[▽]S.-G.J., Y.L., and H-S.J. contributed equally to this work. S.-G.J.: conceptualization, methodology, experiments, data analysis, writing, funding acquisition. Y.L.: conceptualization, methodology, experiments, data analysis, writing. H.-S.J.: conceptualization, methodology, experiments, data analysis, writing. S.J.P.: methodology, data analysis, writing. B.-K.K.: supervision. J.Y.: discussions. C.-H.C.: conceptualization, review & editing, supervision, funding acquisition.

Notes

The authors declare no competing financial interest.

■ ACKNOWLEDGMENTS

This work was supported by the National Research Foundation of Korea (NRF) grant funded by the Korean government: the Ministry of Science and ICT (RS-2024-00346302), and the Ministry of Education (RS-2023-00248536 and no. RS-2023-00301976).

■ REFERENCES

(1) Jusková, P.; Schmitt, S.; Kling, A.; Rackus, D. G.; Held, M.; Egli, A.; Dittrich, P. S. Real-Time Respiration Changes as a Viability Indicator for Rapid Antibiotic Susceptibility Testing in a Microfluidic Chamber Array. *ACS Sens.* **2021**, *6* (6), 2202−2210.

(2) Murray, C. J. L.; Ikuta, K. S.; Sharara, F.; Swetschinski, L.; Robles Aguilar, G.; Gray, A.; Han, C.; Bisignano, C.; Rao, P.; Wool, E.; et al. Global burden of bacterial antimicrobial resistance in 2019: a systematic analysis. *Lancet* **2022**, *399* (10325), 629−655.

(3) Zhang, J.; Wang, M.; Xiao, J.; Wang, M.; Liu, Y.; Gao, X. Metabolism-Triggered Plasmonic Nanosensor for Bacterial Detection and Antimicrobial Susceptibility Testing of Clinical Isolates. *ACS Sens.* **2024**, *9* (1), 379−387.
(4) Georgieva, R.; Yocheva, L.; Tserovska, L.; Zhelezova, G.; Stefanova, N.; Atanasova, A.; Danguleva, A.; Ivanova, G.; Karapetkov, N.; Rumyan, N.; et al. Antimicrobial activity and antibiotic susceptibility of Lactobacillus and Bifidobacterium spp. intended for use as starter and probiotic cultures. *Biotechnol. Biotechnol. Equip.* **2015**, *29* (1), 84−91.
(5) Oliveira, C. P. d.; Silva, J. A. d.; Siqueira-Júnior, J. P. d. Nature of the antimicrobial activity of Lactobacillus casei Bifidobacterium bifidum and Bifidobacterium animalis against foodborne pathogenic and spoilage microorganisms. *Nat. Prod. Res.* **2015**, *29* (22), 2133−2136.
(6) Sabri, M.; El Handi, K.; Calvano, C. D.; Bianco, M.; De Stradis, A.; Valentini, F.; Elbeaino, T. Leuconostoc mesenteroides strain MS4-derived bacteriocins: A potent antimicrobial arsenal for controlling Xylella fastidiosa infection. *Microbiol. Res.* **2025**, *293*, 128071.
(7) Dowdell, P.; Chankhamhaengdecha, S.; Panbangred, W.; Janvilisri, T.; Aroonnual, A. Probiotic activity of Enterococcus faecium and Lactococcus lactis isolated from Thai fermented sausages and their protective effect against Clostridium difficile. *Probiotics Antimicrob. Proteins* **2020**, *12*, 641−648.
(8) Chen, J.; Navarro, E.; Mesich, B.; Gerstbrein, D.; Cruz, A.; Faron, M. L.; Gau, V. Real world clinical feasibility of direct-from-specimen antimicrobial susceptibility testing of clinical specimens with unknown microbial load or susceptibility. *Sci. Rep.* **2022**, *12* (1), 18525.
(9) Hombach, M.; Zbinden, R.; Böttger, E. C. Standardisation of disk diffusion results for antibiotic susceptibility testing using the sirscan automated zone reader. *BMC Microbiol.* **2013**, *13*, 225−8.
(10) Webber, D. M.; Wallace, M. A.; Burnham, C.-A. D. Stop waiting for tomorrow: disk diffusion performed on early growth is an accurate method for antimicrobial susceptibility testing with reduced turnaround time. *J. Clin. Microbiol.* **2022**, *60* (5), e03007−e03020.
(11) Baser, K. H. C.; Buchbauer, G. *Handbook of Essential Oils: Science, Technology, and Applications*; CRC Press, 2009.
(12) Kourmouli, A.; Valenti, M.; van Rijn, E.; Beaumont, H. J.; Kalantzi, O.-I.; Schmidt-Ott, A.; Biskos, G. Can disc diffusion susceptibility tests assess the antimicrobial activity of engineered nanoparticles? *J. Nanopart. Res.* **2018**, *20*, 62−66.
(13) Hombach, M.; Maurer, F. P.; Pfiffner, T.; Böttger, E. C.; Furrer, R. Standardization of operator-dependent variables affecting precision and accuracy of the disk diffusion method for antibiotic susceptibility testing. *J. Clin. Microbiol.* **2015**, *53* (12), 3864−3869.
(14) Mutlu-Ingok, A.; Firtin, B.; Karbancioglu-Guler, F.; Altay, F. A study on correlations between antimicrobial effects and diffusion coefficient, zeta potential and droplet size of essential oils. *Int. J. Food Eng.* **2020**, *16* (11), 20190354.
(15) Klement, E.; Chaffer, M.; Leitner, G.; Shwimmer, A.; Friedman, S.; Saran, A.; Shpigel, N. Assessment of accuracy of disk diffusion tests for the determination of antimicrobial susceptibility of common bovine mastitis pathogens: a novel approach. *Microb. Drug Resist.* **2005**, *11* (4), 342−350.
(16) Coorevits, L.; Boelens, J.; Claeys, G. Direct susceptibility testing by disk diffusion on clinical samples: a rapid and accurate tool for antibiotic stewardship. *Eur. J. Clin. Microbiol. Infect. Dis.* **2015**, *34*, 1207−1212.
(17) Saini, V.; Riekerink, R. O.; McClure, J.; Barkema, H. Diagnostic accuracy assessment of Sensititre and agar disk diffusion for determining antimicrobial resistance profiles of bovine clinical mastitis pathogens. *J. Clin. Microbiol.* **2011**, *49* (4), 1568−1577.
(18) Liu, Y.; Lehnert, T.; Mayr, T.; Gijs, M. A. Antimicrobial susceptibility testing by measuring bacterial oxygen consumption on an integrated platform. *Lab Chip* **2021**, *21* (18), 3520−3531.
(19) Tuomanen, E.; Cozens, R.; Tosch, W.; Zak, O.; Tomasz, A. The rate of killing of Escherichia coli byβ-lactam antibiotics is strictly proportional to the rate of bacterial growth. *Microbiology* **1986**, *132* (5), 1297−1304.
(20) Alonso, A. A.; Molina, I.; Theodoropoulos, C. Modeling bacterial population growth from stochastic single-cell dynamics. *Appl. Environ. Microbiol.* **2014**, *80* (17), 5241−5253.
(21) Svenningsen, M. S.; Mitarai, N. Simple bacterial growth model for the formation of spontaneous and triggered dormant subpopulations. *Phys. Rev. Res.* **2024**, *6* (3), 033072.
(22) Wiegand, I.; Hilpert, K.; Hancock, R. E. Agar and broth dilution methods to determine the minimal inhibitory concentration (MIC) of antimicrobial substances. *Nat. Protoc.* **2008**, *3* (2), 163−175.
(23) Yang, E.; Fan, L.; Jiang, Y.; Doucette, C.; Fillmore, S. Antimicrobial activity of bacteriocin-producing lactic acid bacteria isolated from cheeses and yogurts. *AMB Express* **2012**, *2*, 48−12.
(24) Thuy, T. T. D.; Lu, H.-F.; Bregente, C. J. B.; Huang, F.-C. A.; Tu, P.-C.; Kao, C.-Y. Characterization of the broad-spectrum antibacterial activity of bacteriocin-like inhibitory substance-producing probiotics isolated from fermented foods. *BMC Microbiol.* **2024**, *24* (1), 85.
(25) Dickert, H.; Machka, K.; Braveny, I. The uses and limitations of disc diffusion in the antibiotic sensitivity testing of bacteria. *Infection* **1981**, *9* (1), 18−24.
(26) Beal, J.; Farny, N. G.; Haddock-Angelli, T.; Selvarajah, V.; Baldwin, G. S.; Buckley-Taylor, R.; Gershater, M.; Kiga, D.; Marken, J.; Sanchania, V.; et al. Robust estimation of bacterial cell count from optical density. *Commun. Biol.* **2020**, *3* (1), 512.
(27) Chu, J.-O.; Jeong, H.-S.; Park, J.-P.; Park, K.; Kim, S.-K.; Yi, H.; Choi, C.-H. Capsule-based colorimetric temperature monitoring system for customizable cold chain management. *Chem. Eng. J.* **2023**, *455*, 140753.
(28) Squarzanti, D. F.; Zanetta, P.; Ormelli, M.; Manfredi, M.; Barberis, E.; Vanella, V. V.; Amoruso, A.; Pane, M.; Azzimonti, B. An animal derivative-free medium enhances Lactobacillus johnsonii LJO02 supernatant selective efficacy against the methicillin (oxacillin)-resistant Staphylococcus aureus virulence through key-metabolites. *Sci. Rep.* **2022**, *12* (1), 8666.
(29) Huynh, U.; Qiao, M.; King, J.; Trinh, B.; Valdez, J.; Haq, M.; Zastrow, M. L. Differential effects of transition metals on growth and metal uptake for two distinct Lactobacillus species. *Microbiol. Spectr.* **2022**, *10* (1), e01006−e01021.
(30) Tiwari, D. K.; Jha, G.; Tiwari, M.; Kerkar, S.; Das, S.; Gobre, V. V. Synergistic antibacterial potential and cell surface topology study of carbon nanodots and tetracycline against E. coli. *Front. Bioeng. Biotechnol.* **2021**, *9*, 626276.
(31) Stevenson, K.; McVey, A. F.; Clark, I. B.; Swain, P. S.; Pilizota, T. General calibration of microbial growth in microplate readers. *Sci. Rep.* **2016**, *6* (1), 38828.
(32) Low, H. Z.; Böhnlein, C.; Sprotte, S.; Wagner, N.; Fiedler, G.; Kabisch, J.; Franz, C. M. Fast and easy phage-tagging and live/dead analysis for the rapid monitoring of bacteriophage infection. *Front. Microbiol.* **2020**, *11*, 602444.

https://doi.org/10.1021/acssensors.4c03003
ACS Sens. 2025, 10, 1880−1888